Quark Mass Dependence of Heavy Quark Diffusion Coefficient from Lattice QCD

Luis Altenkort,[1] David de la Cruz,[2] Olaf Kaczmarek,[1] Rasmus Larsen,[3] Guy D. Moore,[2] Swagato Mukherjee,[4] Peter Petreczky,[4] Hai-Tao Shu,[4,*] and Simon Stendebach[2]

(HotQCD Collaboration)

[1]*Fakultät für Physik, Universität Bielefeld, D-33615 Bielefeld, Germany*
[2]*Insitut für Kernphysik, Technische Universität Darmstadt, Schlossgartenstraße 2, D-64289 Darmstadt, Germany*
[3]*Department of Mathematics and Physics, University of Stavanger, Stavanger N-4036, Norway*
[4]*Physics Department, Brookhaven National Laboratory, Upton, New York 11973, USA*

(Received 2 November 2023; revised 24 December 2023; accepted 4 January 2024; published 1 February 2024)

We present the first study of the quark mass dependence of the heavy quark momentum and spatial diffusion coefficients using lattice QCD with light dynamical quarks corresponding to a pion mass of 320 MeV. We find that, for the temperature range 195 MeV $< T <$ 293 MeV, the spatial diffusion coefficients of the charm and bottom quarks are smaller than those obtained in phenomenological models that describe the p_T spectra and elliptic flow of open heavy flavor hadrons.

DOI: 10.1103/PhysRevLett.132.051902

Introduction.—Heavy-ion experiments at high energies hint toward a rapid thermalization of heavy (charm and bottom) quarks. These observations are surprising since the relaxation time of a heavy quark immersed in a quark-gluon plasma (QGP) is expected to be M/T times larger than the relaxation time of the light bulk degrees of freedom constituting the QGP, where M is the heavy quark mass [1,2] and T is the temperature of the QGP. These experimental observations corroborate the picture that the QGP created in such high-energy heavy-ion collisions is an almost perfect fluid, see Refs. [3–5]. This makes the heavy quark diffusion coefficient one of the fundamental transport properties of the QGP, along with other transport coefficients such as shear and bulk viscosities.

The heavy quark momentum diffusion coefficient κ is defined as the average momentum transfer squared to a heavy quark from the medium per unit time, and thus characterizes the kinetic relaxation of heavy quarks toward thermal equilibrium. One can also define the spatial heavy quark diffusion coefficient D_s in terms of the conserved net heavy flavor number through the usual Kubo formula. This spatial heavy quark diffusion coefficient will depend on M, and also has a well defined limit when M goes to zero. Close to equilibrium, in the limit $M \gg T$, the momentum and spatial heavy quark diffusion coefficients are related [2,6],

$$D_s = \frac{2T^2}{\kappa}\frac{\langle p^2\rangle}{3MT}, \tag{1}$$

where $\langle p^2\rangle$ is thermal averaged momentum squared of the heavy quark.

Experimentally measured p_T spectra and the elliptic flows of open charm and open bottom hadrons provide information on the degree of thermalization of the heavy quarks in the QGP, see Refs. [3–5] for reviews. D_s can be estimated by fitting these experimental measurements using phenomenological transport models, see Refs. [3–5]. A key ingredient of these transport models is an effective momentum-dependent heavy-quark diffusion coefficient, which in turn may depend on some effective in-medium cross sections. The D_s appearing in the Kubo formula can be obtained as the zero-momentum limit of this effective diffusion coefficient.

Very recently, D_s has been calculated in $2+1$ flavor QCD for infinitely heavy quarks [7]. This QCD result for the infinite-mass limit turns out to be smaller than the phenomenological estimate of D_s for the charm and bottom quarks. This begs the question of whether or not these discrepancies arise solely due to the mass dependence of D_s. In this Letter, we address this question by presenting first lattice QCD calculations of the mass-dependent D_s with light dynamical quarks.

Theoretical framework.—For $M \gg T$, κ can be calculated using heavy quark effective theory [6,8,9]. In this framework κ is expressed in terms of the correlation

function of chromoelectric (E) and chromomagnetic (B) fields connected by fundamental Wilson lines [6,8,9]. In this effective theory

$$\kappa = \kappa_E + \frac{2}{3}\langle v^2\rangle \kappa_B, \tag{2}$$

where $\kappa_{E,B}(T) = 2T\lim_{\omega\to 0}[\rho_{E,B}(\omega,T)/\omega]$ [6,9], $\rho_{E,B}$ are the spectral functions corresponding to the E and B field correlation functions, and $\langle v^2\rangle$ is the mean-squared thermal velocity of the heavy quark [6]. The quark mass dependence of κ enters through $\langle v^2\rangle$. At the leading order in $1/M$, $\langle v^2\rangle = 3T/M$. In this way, κ_B controls the quark mass dependence of κ.

Lattice QCD calculations of κ_B rely on accessing $\rho_B(\omega,T)$ from the correlator [6]

$$G_B(\tau,T) = \sum_{i=1}^{3} \frac{\langle \mathrm{ReTr}[U(\beta,\tau)B_i(\mathbf{x},\tau)U(\tau,0)B_i(\mathbf{x},0)]\rangle}{3\langle \mathrm{ReTr}U(\beta,0)\rangle}, \tag{3}$$

where $\beta = 1/T$ is the inverse temperature, τ is the Euclidean time separation of the B operators, and $U(\tau_1,\tau_2)$ is a thermal Wilson line connecting the B fields located at Euclidean times τ_1 and τ_2. ρ_B is related to $G_B(\tau,T)$ via the integral equation

$$G_B(\tau,T) = \int_0^\infty \frac{\mathrm{d}\omega}{\pi}\rho_B(\omega,T)\frac{\cosh[\omega\tau - \omega/(2T)]}{\sinh[\omega/(2T)]}. \tag{4}$$

Lattice QCD setup.—In the present calculation we use the same lattice QCD setup and ensembles that were used for the calculation of κ_E [7], specifically, $2+1$ flavors of quarks in the highly improved staggered quark fermionic action [10] and the tree-level improved Lüscher-Weisz gauge action [11,12] with physical values of the kaon and 320 MeV pion masses and at $T = 195$, 220, 251, and 293 MeV. At each temperature we use three lattice spacings (a) to carry out continuum extrapolations ($a \to 0$) of G_B. Further details are provided in Supplemental Material [13].

The B fields are discretized on the lattice as $B_i(\mathbf{x}) \equiv \epsilon_{ijk}\big(U_j(\mathbf{x})U_k(\mathbf{x}+\hat{j}) - U_k(\mathbf{x})U_j(\mathbf{x}+\hat{k})\big)/2$. For measurements of G_B we use a Symanzik-improved version [34] of gradient flow [35–38]. Guided by our experience [14,15] and perturbative QCD (pQCD) [39] we limit the gradient-flow time (τ_F) within the range $\sqrt{8\tau_\mathrm{F}} < \tau/3$. We find that gradient flow improves the signal-to-noise ratio of G_B.

At 1-loop level [40] in pQCD G_B has a nontrivial anomalous dimension, and gradient flow serves as a nonperturbative renormalization scheme for G_B. The continuum-extrapolated G_B are renormalized in the gradient-flow scheme at the scale $\mu_\mathrm{F} = 1/\sqrt{8\tau_\mathrm{F}}$. The renormalization-group invariant physical correlator, G_B^phys, is obtained via the one-loop pQCD matching [16]

$$G_B^\mathrm{phys}(\tau,T) = \lim_{\tau_\mathrm{F}\to 0} Z_\mathrm{match}(\bar{\mu}_T,\bar{\mu}_{\tau_\mathrm{F}},\mu_\mathrm{F})G_B(\tau,T,\tau_\mathrm{F}). \tag{5}$$

The power-law corrections arising from mixing with high-dimension operators are removed through the $\tau_\mathrm{F}\to 0$ extrapolations at each T. The matching function, Z_match, involves three components: matching from the gradient flow to the $\overline{\mathrm{MS}}$ scheme at a scale $\bar{\mu}_{\tau_\mathrm{F}}$, matching between $\overline{\mathrm{MS}}$-renormalized thermal QCD to the static quark effective theory at a scale $\bar{\mu}_T$, and running of the anomalous dimension of the operator from $\bar{\mu}_T$ to $\bar{\mu}_{\tau_\mathrm{F}}$. If Z_match were known up to all orders in pQCD, the dependence of G_B^phys on the scales $\bar{\mu}_T$ and $\bar{\mu}_{\tau_\mathrm{F}}$ would exactly cancel. Since Z_match is known only up to one loop (NLO), we estimate the uncertainty from unknown higher-order effects in the matching by varying the values of each scale; for $\bar{\mu}_T$ we consider the two choices $\bar{\mu}_T = 2\pi T$ or $19.18T$, and for $\bar{\mu}_{\tau_\mathrm{F}}$ we consider $\bar{\mu}_{\tau_\mathrm{F}} = \mu_\mathrm{F}$ or $1.4986\mu_\mathrm{F}$. Further details and the expression for Z_match are given in Supplemental Material [13].

Data analysis.—To estimate the physical B-field correlator from lattice calculations we first have to take the continuum limit of the correlation function calculated at a given flow time. The B-field correlator G_B scales with a strong negative power of τ since $\rho_B \propto \omega^3$ at large ω. To mitigate this as well as the lattice artifacts and distortion due to gradient flow [7] we normalize G_B with $G^\mathrm{norm}(\tau,T,N_\tau,\tau_\mathrm{F}) = G_B^\mathrm{LO}(\tau,T,N_\tau,\tau_\mathrm{F})/(C_F g^2)$, where G_B^LO is the tree-level pQCD results for G_B at nonzero lattice spacing and gradient-flow time, C_F is the Casimir factor, and g^2 is the strong coupling. For brevity we suppress the arguments of the normalization correlator.

Our lattice data are not $G_B(\tau,T,\tau_\mathrm{F})$ directly, but $G_B(\tau,T,N_\tau,\tau_\mathrm{F})$ with N_τ the number of points across the lattice time direction, which is related to the lattice spacing via $N_\tau a = 1/T$. Therefore, before performing the $\tau_\mathrm{F}\to 0$ limit in Eq. (5), we must first take the $N_\tau\to\infty$ limit to find $G_B(\tau,T,\tau_\mathrm{F})$. Because the available τ values also depend on the lattice spacing, we first perform a τ interpolation of $G_B(\tau,T,N_\tau,\tau_\mathrm{F})/G^\mathrm{norm}$ on the two coarsest lattices, separately at each (T,τ_F) pair, to establish the value at the τ values available on the finest lattice. This then allows the $N_\tau\to\infty$ extrapolation, which is performed independently at each (τ,T,τ_F) triple. In extrapolating to $N_\tau\to\infty$ we assume that the discretization errors scale as $1/N_\tau^2 = (aT)^2$.

For each τT, to take the $\tau_\mathrm{F}\to 0$ limit we multiply the continuum-extrapolated results for G_B/G^norm by Z_match and do linear extrapolations in τ_F, as suggested by NLO pQCD [41]. To avoid potentially large discretization effects and to keep the gradient-flow scale smaller than all relevant physical scales in the problem, we restrict to the range of flow times $0.25 \le \sqrt{8\tau_\mathrm{F}}/\tau \le 0.30$ [7].

As an example, in Fig. 1 (left panel) we show the resulting G_B^phys for different choices of $\bar{\mu}_{\tau_\mathrm{F}}$ and $\bar{\mu}_T$. In Fig. 1 (right panel) we show the T dependence of G_B^phys for $\bar{\mu}_T/T = 19.18$ and $\bar{\mu}_{\tau_\mathrm{F}}/\mu_\mathrm{F} = 1.0$. Further details on and

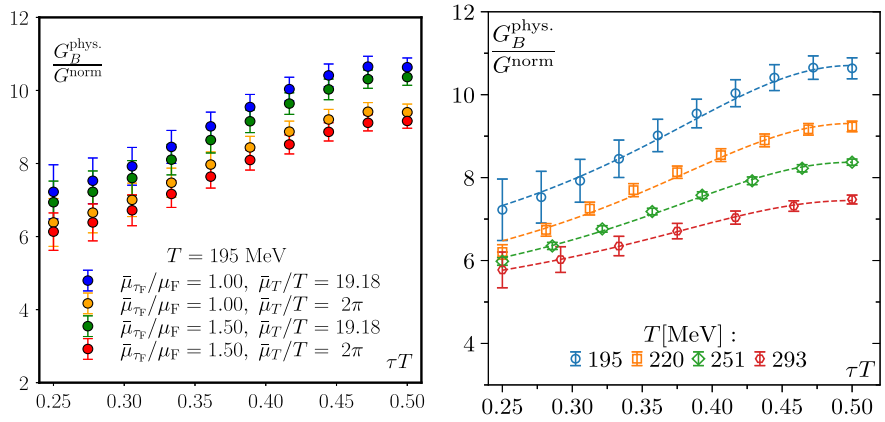

FIG. 1. Left: Scale dependence of G_B^{phys} [cf Eq. (5)] at $T = 195$ MeV. Right: Temperature dependence of G_B^{phys} for $\bar{\mu}_T/T = 19.18$ and $\bar{\mu}_{\tau_F}/\mu_F = 1.0$. The dashed curves denote the central values of the smax model fit to G_B^{phys} with NLO ρ_{uv} at scale $\mu = \sqrt{(0.133\,06\omega)^2 + \mu_{\text{DR}}^2}$.

examples of G_B^{phys} can be found in Supplemental Material [13].

G_B^{phys} are fitted to Eq. (4) to obtain κ_B. κ_B is encoded in the infrared region of the spectral function, $\rho_B^{\text{ir}}(\omega) = \omega\kappa_B/(2T)$. For the ultraviolet region of spectral function, $\rho_B^{\text{uv}}(\omega,\mu)$, we use leading order and NLO vacuum pQCD results. To convert the NLO pQCD results [16,17] from the $\overline{\text{MS}}$ scheme, at the scale μ, to the renormalization-group invariant physical scheme we use the matching NLO Wilson coefficient [18], $c_B^2(\mu,\bar{\mu}_T)$, to the static quark effective theory. To account for possible higher order effects we also introduce another (in addition to κ_B) ω-independent fit parameter, K. The resulting choices for the UV part of the physical spectral function are $\rho_B^{\text{uv,phys}}(\omega) = \{K\rho_B^{\text{uv,LO}}(\omega,\mu), Kc_B^2(\mu,\bar{\mu}_T)\rho_B^{\text{uv,NLO}}(\omega,\mu)\}$. Expressions for $\rho^{\text{uv,LO}}$, $\rho^{\text{uv,NLO}}$, and $c_B^2(\mu,\bar{\mu}_T)$ are given in Supplemental Material [13].

Following the previous works [7,14,19,42] we use three models to interpolate between ρ_B^{ir} and ρ_B^{uv} to obtain ρ_B over all ω. (1) The maximum (max) model, $\rho_{\text{max}} = \max\left(\rho_B^{\text{ir}}(\omega), \rho_B^{\text{uv,phys}}(\omega)\right)$, which imposes a hard switchover between the two regimes. (2) The smooth maximum (smax) model, $\rho_{\text{smax}} = \sqrt{(\rho_B^{\text{ir}}(\omega))^2 + (\rho_B^{\text{uv,phys}}(\omega))^2}$, which imposes a smooth switchover. (3) The power-law (plaw) model, ρ_{plaw}, which is $\rho_B^{\text{ir}}(\omega)$ up to $\omega = \omega_{\text{ir}}$ and $\rho_B^{\text{uv,phys}}(\omega)$ above $\omega = \omega^{\text{uv}}$. In between, it is connected by a power-law curve $\rho_B(\omega) = c\,\omega^p$. The parameters c and p are chosen to provide continuity at the boundary. Physically motivated choices of these boundaries are $\omega_{\text{ir}} = T$ and $\omega_{\text{uv}} = 2\pi T$ [7].

ρ_{max}, ρ_{smax}, and ρ_{plaw} also depend on the intermediate $\overline{\text{MS}}$ renormalization scale μ. For reasons discussed in Supplemental Material [13], we consider two options $\mu = \sqrt{(0.13306\omega)^2 + \mu_{\text{DR}}^2}$ and $\mu = \sqrt{4\omega^2 + \mu_{\text{DR}}^2}$, where $\mu_{\text{DR}} \approx 9.1T$ is a typical thermal scale inferred from the high temperature three dimensional effective theory [20].

Results.—Combining different choices of (1) $\bar{\mu}_T$ and $\bar{\mu}_{\tau_F}$ in G_B^{phys}, (2) $\rho_B^{\text{uv,phys}}(\omega,\mu)$ and μ, and (3) three interpolating models ρ_{max}, ρ_{smax}, and ρ_{plaw}, we carry out 24 different fits for K and κ_B on each bootstrap sample of gauge configurations at each T. The final result for κ_B at each T is obtained from the median and 68% confidence limit of the distribution of all the bootstrap samples over gauge configurations and fit forms and, thus, include both statistical as well as systematic errors arising from different model and scales choices. We find $\kappa_B(T = 195\,\text{MeV}) = 10.42^{+2.66}_{-3.61}T^3$, $\kappa_B(T = 220\ \text{MeV}) = 8.78^{+2.20}_{-3.21}T^3$, $\kappa_B(T = 251\ \text{MeV}) = 7.18^{+1.94}_{-2.90}T^3$, and $\kappa_B(T = 293\ \text{MeV}) = 5.02^{+1.92}_{-2.24}T^3$, which are of similar magnitude to κ_E obtained for the same ensembles [7]. The κ_B for $2+1$ flavor QCD turns out be much larger than those from quenched QCD [15,17] at the same values of T/T_c. For further details on the fits and results see Supplemental Material [13].

The $\langle v^2\rangle$ appearing in Eq. (2) can be obtained either from the low-frequency part of the spectral function corresponding to the net-flavor current [9,43] or in the quasiparticle model with a temperature dependent quark mass [21]. In quenched QCD it has been shown that a quasiparticle model with a temperature dependent heavy quark mass fitted to the heavy quark number susceptibility gives a $\langle v^2\rangle$ that agrees with the one obtained from the low-frequency part of the net heavy quark current spectral function [21]. Therefore, in this work we adopt the quasiparticle model to calculate $\langle v^2\rangle$. For the temperature dependent charm quark is obtained from the continuum-extrapolated lattice QCD results for the charm susceptibility [22]. No lattice QCD results for bottom quark susceptibility are available presently. Therefore, we simply fix the effective bottom quark mass to 4.8 GeV. The $\langle p^2\rangle$ needed to obtain D_s, cf. Eq. (1), are estimated from the quasiparticle model in the same way as for the $\langle v^2\rangle$. For further details, see Supplemental Material [13]. There we also show that the $\langle v^2\rangle$, $\langle p^2\rangle$ and the values of D_s are not too sensitive to the precise choice of the bottom quark mass.

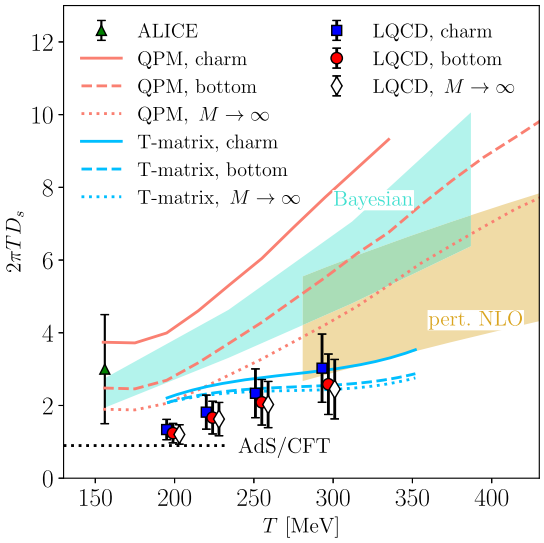

FIG. 2. Lattice QCD (LQCD) results for the spatial diffusion coefficients D_s for the charm, bottom, and infinitely heavy quarks compared with those from the quasiparticle model (QPM) [44] and the T-matrix approach [45,46]. Also shown are the infinitely heavy quark diffusion coefficients from the ALICE Collaboration's phenomenological estimate [47,48], NLO perturbative calculation [49], and AdS/CFT estimate at a certain value of λ [8]. The width of the NLO perturbative QCD band corresponds to the variation of the renormalization scale from $\mu = 2\pi T$ (upper boundary of the orange band) and $\mu = 4\pi T$ (lower boundary).

Final results for D_s are summarized in Fig. 2. We find a slight increase in D_s with decreasing heavy quark mass. We compare our results with those obtained from a phenomenological quasiparticle model (QPM) [44] and the T-matrix approach [45,46]. We find that D_s in QCD is smaller than the results of these calculations and shows smaller dependence on the heavy quark mass, with the exception of the T-matrix result at the highest temperature considered by us. Our result for D_s is also smaller than other phenomenological estimates [47,48], which do not take into account the quark mass dependence. Finally, for completeness, we show the AdS/CFT estimate [8] of D_s with a certain value of λ and the result of the NLO perturbative calculation [49] in the limit $M \to \infty$.

Conclusion.—We presented the $2 + 1$ flavor lattice QCD calculations of the quark mass dependence of the momentum and spatial heavy quark diffusion coefficients. In the temperature range $195\ \text{MeV} \leq T \leq 293\ \text{MeV}$ the quark mass dependence turns out to be quite small. In conjunction with the previous results for an infinitely heavy quark [7], the present calculations provide the first nonperturbative QCD results for the charm and bottom quark diffusion coefficients in the QGP. These nonperturbative QCD results will serve as critical inputs to and benchmarks for various dynamical models to study thermalization of charm and bottom quarks in the strongly coupled medium created in heavy-ion collisions at the Large Hadron Collider and the Relativistic Heavy-Ion Collider.

All computations in this work were performed using SIMULATeQCD [50–52].

All data from our calculations, presented in the figures of this Letter, can be found in [53].

This material is based upon work supported by the U.S. Department of Energy, Office of Science, Office of Nuclear Physics through Contract No. DE-SC0012704, and within the frameworks of Scientific Discovery through Advanced Computing (SciDAC) award *Fundamental Nuclear Physics at the Exascale and Beyond* and the Topical Collaboration in Nuclear Theory *Heavy-Flavor Theory (HEFTY) for QCD Matter*. This work is supported by the Deutsche Forschungsgemeinschaft (DFG, German Research Foundation) through the CRC-TR 211 "Strong-interaction matter under extreme conditions"—Project No. 315477589—TRR 211. R. L. acknowledges funding by the Research Council of Norway under the FRIPRO Young Research Talent Grant No. 286883. We thank Szabolcs Borsányi for providing the continuum extrapolated data for charm susceptibility. This research used awards of computer time provided by the ALCC program at the Oak Ridge Leadership Computing Facility, which is a DOE Office of Science User Facility supported under Contract No. DE-AC05-00OR22725; the National Energy Research Scientific Computing Center (NERSC), a U.S. Department of Energy Office of Science User Facility located at Lawrence Berkeley National Laboratory, operated under Contract No. DE-AC02- 05CH11231; the PRACE awards on JUWELS at GCS@FZJ, Germany and Marconi100 at CINECA, Italy. Computations for this work were carried out in part on facilities of the USQCD Collaboration, which are funded by the Office of Science of the U.S. Department of Energy. Parts of the computations in this work also were performed at Bielefeld University's GPU Cluster, supported by the North Rhine-Westphalian competence network for high-performance computing (HPC.NRW).

*hshu@bnl.gov

[1] B. Svetitsky, Phys. Rev. D **37**, 2484 (1988).
[2] G. D. Moore and D. Teaney, Phys. Rev. C **71**, 064904 (2005).
[3] A. Beraudo *et al.*, Nucl. Phys. **A979**, 21 (2018).
[4] X. Dong, Y.-J. Lee, and R. Rapp, Annu. Rev. Nucl. Part. Sci. **69**, 417 (2019).
[5] M. He, H. van Hees, and R. Rapp, Prog. Part. Nucl. Phys. **130**, 104020 (2023).
[6] A. Bouttefeux and M. Laine, J. High Energy Phys. 12 (2020) 150.
[7] L. Altenkort, O. Kaczmarek, R. Larsen, S. Mukherjee, P. Petreczky, H.-T. Shu, and S. Stendebach (HotQCD Collaborations), Phys. Rev. Lett. **130**, 231902 (2023).
[8] J. Casalderrey-Solana and D. Teaney, Phys. Rev. D **74**, 085012 (2006).
[9] S. Caron-Huot, M. Laine, and G. D. Moore, J. High Energy Phys. 04 (2009) 053.

[10] E. Follana, Q. Mason, C. Davies, K. Hornbostel, G. P. Lepage, J. Shigemitsu, H. Trottier, and K. Wong (HPQCD, UKQCD Collaborations), Phys. Rev. D **75**, 054502 (2007).

[11] M. Luscher and P. Weisz, Commun. Math. Phys. **97**, 59 (1985); **98**, 433(E) (1985).

[12] M. Luscher and P. Weisz, Phys. Lett. **158B**, 250 (1985).

[13] See Supplemental Material at http://link.aps.org/supplemental/10.1103/PhysRevLett.132.051902 for the technical details of this study, which includes Refs. [7,9,14–33].

[14] L. Altenkort, A. M. Eller, O. Kaczmarek, L. Mazur, G. D. Moore, and H.-T. Shu, Phys. Rev. D **103**, 014511 (2021).

[15] N. Brambilla, V. Leino, J. Mayer-Steudte, and P. Petreczky (TUMQCD Collaboration), Phys. Rev. D **107**, 054508 (2023).

[16] D. d. l. Cruz and G. D. Moore (to be published).

[17] D. Banerjee, S. Datta, and M. Laine, J. High Energy Phys. 08 (2022) 128.

[18] M. Laine, J. High Energy Phys. 06 (2021) 139.

[19] N. Brambilla, V. Leino, P. Petreczky, and A. Vairo, Phys. Rev. D **102**, 074503 (2020).

[20] K. Kajantie, M. Laine, K. Rummukainen, and M. E. Shaposhnikov, Nucl. Phys. **B503**, 357 (1997).

[21] P. Petreczky, Eur. Phys. J. C **62**, 85 (2009).

[22] R. Bellwied, S. Borsanyi, Z. Fodor, S. D. Katz, A. Pasztor, C. Ratti, and K. K. Szabo, Phys. Rev. D **92**, 114505 (2015).

[23] S. Stendebach, Perturbative analysis of operators under improved gradient flow in lattice QCD, Master's thesis, Technische Universität Darmstadt, 2022.

[24] D. Banerjee, R. Gavai, S. Datta, and P. Majumdar, Nucl. Phys. **A1038**, 122721 (2023).

[25] A. Bazavov and P. Petreczky (HotQCD Collaboration), J. Phys. Conf. Ser. **230**, 012014 (2010).

[26] A. Bazavov, P. Petreczky, and J. H. Weber, Phys. Rev. D **97**, 014510 (2018).

[27] K. G. Chetyrkin, J. H. Kuhn, and M. Steinhauser, Comput. Phys. Commun. **133**, 43 (2000).

[28] M. A. Clark and A. D. Kennedy, Nucl. Phys. B, Proc. Suppl. **129**, 850 (2004).

[29] M. A. Clark, A. D. Kennedy, and Z. Sroczynski, Nucl. Phys. B, Proc. Suppl. **140**, 835 (2005).

[30] Y. Aoki *et al.* (Flavour Lattice Averaging Group (FLAG) Collaboration), Eur. Phys. J. C **82**, 869 (2022).

[31] F. Herren and M. Steinhauser, Comput. Phys. Commun. **224**, 333 (2018).

[32] A. Bazavov, T. Bhattacharya, C. DeTar, H. T. Ding, S. Gottlieb *et al.* (HotQCD Collaboration), Phys. Rev. D **90**, 094503 (2014).

[33] A. Bazavov *et al.* (MILC Collaboration), Proc. Sci. LATTICE2010 (**2010**) 074.

[34] A. Ramos and S. Sint, Eur. Phys. J. C **76**, 15 (2016).

[35] R. Narayanan and H. Neuberger, J. High Energy Phys. 03 (2006) 064.

[36] M. Lüscher, Commun. Math. Phys. **293**, 899 (2010).

[37] M. Lüscher, J. High Energy Phys. 08 (2010) 071; 03 (2014) 092(E).

[38] M. Lüscher and P. Weisz, J. High Energy Phys. 02 (2011) 051.

[39] A. M. Eller and G. D. Moore, Phys. Rev. D **97**, 114507 (2018).

[40] E. Eichten and B. R. Hill, Phys. Lett. B **243**, 427 (1990).

[41] A. M. Eller, The color-electric field correlator under gradient flow at next-to-leading order in quantum chromodynamics, Ph.D. thesis, Technische Universität Darmstadt, 2021.

[42] A. Francis, O. Kaczmarek, M. Laine, T. Neuhaus, and H. Ohno, Phys. Rev. D **92**, 116003 (2015).

[43] Y. Burnier and M. Laine, J. High Energy Phys. 11 (2012) 086.

[44] M. L. Sambataro, V. Minissale, S. Plumari, and V. Greco, arXiv:2304.02953.

[45] S. Y. F. Liu and R. Rapp, Eur. Phys. J. A **56**, 44 (2020).

[46] Z. Tang, S. Mukherjee, P. Petreczky, and R. Rapp, arXiv:2310.18864.

[47] Y. Xu, J. E. Bernhard, S. A. Bass, M. Nahrgang, and S. Cao, Phys. Rev. C **97**, 014907 (2018).

[48] S. Acharya *et al.* (ALICE Collaboration), J. High Energy Phys. 01 (2022) 174.

[49] S. Caron-Huot and G. D. Moore, Phys. Rev. Lett. **100**, 052301 (2008).

[50] L. Mazur, Topological aspects in lattice QCD, Ph.D. thesis, Bielefeld University, 2021.

[51] D. Bollweg, L. Altenkort, D. A. Clarke, O. Kaczmarek, L. Mazur, C. Schmidt, P. Scior, and H.-T. Shu, Proc. Sci. LATTICE2021 (**2022**) 196.

[52] L. Mazur *et al.* (HotQCD Collaboration), arXiv:2306.01098.

[53] L. Altenkort, O. Kaczmarek, R. Larson, S. Mukherjee, P. Petreczky, H.-T. Shu, and S. Stendebach, Data publication: Quark Mass Dependence of Heavy Quark Diffusion Coefficient from Lattice QCD (2023), 10.4119/unibi/2979080.